

Effects of false vocal fold adduction and aryepiglottic sphincter narrowing on the voice source in a three-dimensional voice production model

Tsukasa Yoshinaga^{1,2,a}  and Zhaoyan Zhang^{1,b} 

¹School of Medicine, University of California, Los Angeles, 1000 Veteran Avenue, Los Angeles, California 90024, USA

²Graduate School of Engineering Science, Osaka University, 1-3 Machikaneyama, Toyonaka, 560-8531, Japan

ABSTRACT:

Although voice production often involves false vocal fold (FVF) adduction and aryepiglottic sphincter (AES) narrowing, their effects on the voice source still remain unclear. In this study, a three-dimensional (3D) compressible flow simulation coupled to a two-mass vocal fold model in a vocal tract with varying degrees of constriction at the levels of the FVF and AES is conducted. Results showed a small effect of FVF adduction and AES narrowing on the voice source except when the FVFs were strongly adducted. Strong FVF adduction reduced the glottal resistance and increased the transglottal pressure, thus strengthening the voice source. This reduction in glottal resistance is a result of the glottal jet persisting longer into the supraglottal region, which can be achieved by constricting the jet from the medial-lateral direction. In contrast, constricting the jet flow from the anterior-posterior direction had almost no influence on the source strength. In summary, the effect of the 3D supraglottal flow features on the voice source is small except for extreme FVF adduction, and the effect of epilaryngeal adduction is mainly on the vocal tract transfer function rather than the voice source. © 2025 Acoustical Society of America. <https://doi.org/10.1121/10.0036359>

(Received 1 July 2024; revised 14 February 2025; accepted 17 March 2025; published online 2 April 2025)

[Editor: James F. Lynch]

Pages: 2408–2421

I. INTRODUCTION

Human voice is produced by a fluid-structure interaction between the elastic vocal folds in the larynx and airflow from the lungs. The oscillation of vocal folds modulates the airflow into a pulsating jet flow, which is considered to be the primary sound source in phonation. Immediately above the vocal folds, there is a pair of false vocal folds (FVFs), whose adduction may constrict the flow channel along the medial-lateral direction. The space between the vocal folds and FVFs is called the ventricle, also known as *sinus of Morgagni*. Another constriction to the airflow may also be formed at the level of the aryepiglottic folds because of the contraction of the aryepiglottic sphincter (AES), which approximates the epiglottis and arytenoids and constricts the airflow mostly along the anterior-posterior direction. The FVFs and the AES form the epilarynx tube. Manipulation of epilarynx tube dimensions is known to play an important role in producing different voice quality (e.g., Sundberg, 1974; Yanagisawa *et al.*, 1989; Titze and Worley, 2009; Moisiuk and Esling, 2014; Jelinger *et al.*, 2024). This topic has been the focus of many previous studies. However, the effect of epilaryngeal constrictions on the voice source (the time derivative of volume flow rate at the glottis) still remains unclear.

The acoustic effects of epilarynx manipulation on vocal tract transfer function are generally well understood. Sundberg (1974) showed that the relationship of the cross-sectional areas among pharynx, ventricle space, and sinus piriformis plays an important role in clustering third to fifth formants, resulting in a spectral envelop peak around 3 kHz, which is also known as the singer's formant clustering. In addition, a series of studies reported inter-speaker variability of laryngeal tube sizes and its effects on the vocal tract acoustic resonances (Takemoto *et al.*, 2006; Honda *et al.*, 2010; Zhang *et al.*, 2019). They found that female subjects had smaller epilaryngeal tubes than males, which increased formant amplitudes around 3–3.5 kHz in males and 3.5–4 kHz in females.

From the aerodynamic point of view, the presence of non-vibrating FVFs has been shown to reduce glottal jet deflection and glottal flow resistance in numerical flow simulations (e.g., Zhang *et al.*, 2002; Zheng *et al.*, 2009; Xue and Zheng, 2017). Glottal resistance measures the opposition to airflow through the vocal folds and is defined as the transglottal pressure, which is the pressure difference between the subglottal and supraglottal regions divided by the glottal flow rate. Previous studies have investigated the effects of FVF dimensions (e.g., the FVF gap, distance from the vocal folds, and depth of the ventricular space) on the glottal flow. Some studies have examined these effects using flow simulations with rigid vocal fold models (Farahani *et al.*, 2013; Mihaescu *et al.*, 2013; Farbos de Luzan *et al.*, 2015), whereas others have considered vocal folds with forced

^aEmail: yoshinaga.tsukasa.es@osaka-u.ac.jp

^bEmail: zy Zhang@ucla.edu

oscillation (Sadeghi *et al.*, 2019). It should be noted that the above flow simulations solved the incompressible flow equations and did not consider the interaction with vocal tract acoustics. The effects of FVF adduction on voice production have also been investigated experimentally using rigid and silicone vocal fold models (Agarwal *et al.*, 2004; Kucinschi *et al.*, 2006; Bailly *et al.*, 2008; Kniesburges *et al.*, 2017), whereas the effects of AES narrowing have been studied in excised larynges (Alipour *et al.*, 2007; Döllinger *et al.*, 2012). These experimental studies suggested that the glottal flow resistance depends on the ratio of glottal gaps to the FVF gaps. When the FVF gap is approximately eight times or more than the glottal gap, the flow resistance remains the same; but if the ratio is less than eight and greater than one, the FVFs reduce the resistance (Agarwal *et al.*, 2004).

A numerical simulation by Titze and Story (1997) showed that the epilaryngeal narrowing may lower phonation threshold pressure and increase the glottal flow amplitudes. Further analysis by Titze (2006) showed that vocal efficiency and vocal economy can be improved by vocal tract exercises, targeting constrictions at the epilarynx and lips. Such exercises are often targeted in voice training and voice therapy (e.g., the semi-occluded vocal tract) to improve voice production and minimize the risk of vocal fold injury. However, it is often unclear whether the improvement in vocal efficiency is a result of an improvement in the voice source as a result of source-filter interaction or simply an improvement in the acoustic (filtering) effect of the vocal tract (e.g., Sundberg, 1974).

A recent simulation study (Zhang, 2023) demonstrated that the effects of epilaryngeal constriction on the voice source were relatively small and argued that improvement of vocal efficiency associated with epilaryngeal constriction was mainly because of changes in vocal tract acoustics rather than improved voice production at the glottis. Moreover, the effect of vocal tract adjustments on the vocal fold contact pressure was found to be generally small (Zhang, 2021a,b). However, these simulation studies used a one-dimensional (1D) flow model and ignored the three-dimensional (3D) nature of the glottal flow, which may impact the voice source differently from those predicted from a 1D flow model. Narrowing of the AES constricts the airflow mostly from the anterior-posterior direction, whereas the FVF adduction constricts the airflow from the medial-lateral direction. Thus, it is also possible that FVF and AES constrictions may impact the voice source differently.

The goal of this study is to clarify the effects of epilaryngeal constrictions at the levels of the FVF and AES on the voice source and radiated voice outside the mouth in a 3D voice production model. To investigate the potential 3D flow effects, we coupled a 3D compressible flow simulation to a two-mass model of the vocal folds. By changing the degree, location, and orientation of epilaryngeal constriction, we quantify the effects of epilaryngeal constrictions on the 3D flow field, voice source, and radiated sound. Another focus of this study is to compare vocal fold contact pressure

at different epilaryngeal configurations and clarify the impact of epilaryngeal constriction on the risk of vocal fold injury and vocal health.

II. METHODS

A 3D compressible flow simulation coupled with a two-mass model of the vocal folds was conducted in this study. The use of a two-mass model for the vocal folds was to avoid the high computational costs associated with modeling the 3D vocal fold vibrations. In addition, a simplified geometry of the vocal tract and epilaryngeal constriction was used to focus on the effects of constriction size, orientation, and location. The simplified vocal tract is displayed in Fig. 1. The overall flow channel, including an inlet pressure chamber and subglottal and supraglottal tracts, was simplified with rectangular ducts. The inlet pressure chamber had a volume of 163 cm^3 , and a constant pressure was imposed at the inlet to mimic airflow from the lungs. The sub- and supraglottal tracts had a cross-sectional area of $17 \times 17 \text{ mm}^2$ and lengths of 150 and 175 mm, respectively. These dimensions were determined based on typical values of males (Stevens, 1998). The origin of the coordinate along the flow direction ($x=0$) was set at the superior surface of the vocal folds.

To simulate the 3D glottal flow, two masses for the vocal folds were represented by two aligned cylinders (Fig. 1), and the cylinder surfaces were connected with smooth walls as in Pelorson *et al.* (1994). The lower and upper masses had diameters of $d_1=2.5 \text{ mm}$ and $d_2=0.5 \text{ mm}$, respectively. The lateral walls of the vocal folds extended inferiorly to $x=-9 \text{ mm}$. Downstream from the vocal folds, constrictions were formed at the levels of the FVFs and AES, as depicted in Figs. 1(b) and 1(c). The FVFs had a vertical thickness of $t_{\text{FVF}}=4 \text{ mm}$, and the narrowest FVF constrictions were located at a distance $d_{\text{FVF}}=4 \text{ mm}$ downstream from the superior surface of the vocal folds. The FVFs formed a rectangular constriction with medial-lateral and anterior-posterior dimensions, $g_{\text{FVF_ML}}$ and $g_{\text{FVF_AP}}$, respectively. The AES constriction had a vertical thickness of $t_{\text{ML}}=8 \text{ mm}$, and the narrowest point of the AES was located at a distance $d_{\text{AES}}=12 \text{ mm}$ downstream from the superior surface of the vocal folds, forming a rectangular constriction with the dimensions of $g_{\text{AES_ML}}$ and $g_{\text{AES_AP}}$.

In this study, five vocal tract configurations were investigated. The first and second configurations considered constrictions at the level of the FVFs and AES alone, respectively (cases 1 and 2; also see Fig. 1). In each case, the constriction gap was varied from 3 to 13 mm (Table I) along the medial-lateral direction at the FVF level and the anterior-posterior direction at the AES level. Assuming a mean glottal gap of 1 mm, this corresponds to a ratio between the constriction gap and glottal gap from 3 to 13. The gap ranges were determined based on the observation by Agarwal *et al.* (2004). Examples of the vocal tract cross-sectional areas for different degrees of constrictions at the

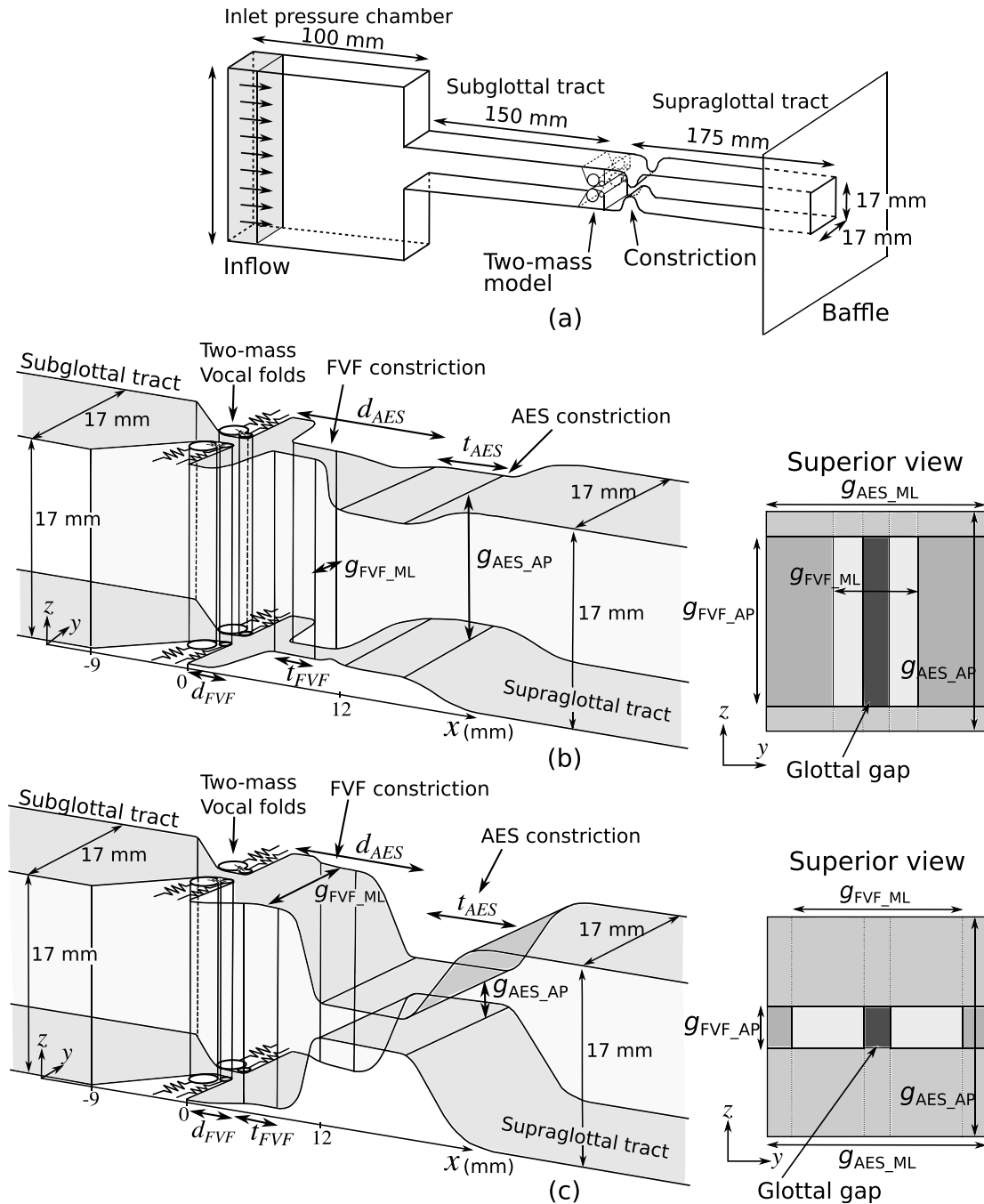


FIG. 1. Geometry of the simulation domain. (a) The overall flow channel; (b) vocal tract with constriction at the level of the FVFs alone, where $d_{FVF} = 4$ mm and $t_{FVF} = 4$ mm; and (c) vocal tract with constriction at the level of the AES alone, where $d_{AES} = 12$ mm and $t_{AES} = 8$ mm, are shown.

levels of the FVFs and AES are plotted in Figs. 2(a) and 2(b).

FVF adduction and AES narrowing differ in the distance from the vocal folds and the constriction direction: FVF adduction constricts the airflow from the medial-lateral direction, whereas the AES narrowing constricts the airflow mostly from the anterior-posterior direction. To isolate the effects of constriction distance and constriction direction, two additional vocal tract configurations were considered in this study. In case 3, a constriction of varying degree was

formed at the level of the FVFs to constrict the airway from the anterior-posterior direction. In case 4, a constriction of varying degree was formed at the level of the AES to constrict the airway from the medial-lateral direction. Finally, in the fifth configuration (case 5), constrictions of varying degree were formed at the levels of both the FVF (from the medial-lateral direction) and AES (from the anterior-posterior direction), simulating conditions of simultaneous FVF adduction and AES narrowing [see the cross-sectional areas in Fig. 2(c)]. The constriction dimensions for each

TABLE I. Dimensions of vocal tract constriction at the levels of the FVF and AES in the five simulation cases.

| | FVF constriction | | AES constriction | |
|--|--------------------|--------------------|--------------------|--------------------|
| | g_{FVF_ML} (mm) | g_{FVF_AP} (mm) | g_{AES_ML} (mm) | g_{AES_AP} (mm) |
| Without constriction | 13 | 17 | 17 | 13 |
| FVF-ML (case 1) | 9 | 17 | 17 | 13 |
| | 7 | 17 | 17 | 13 |
| | 5 | 17 | 17 | 13 |
| | 3 | 17 | 17 | 13 |
| AES_AP (case 2) | 13 | 17 | 17 | 9 |
| | 13 | 17 | 17 | 7 |
| | 13 | 17 | 17 | 5 |
| | 13 | 17 | 17 | 3 |
| FVF_AP (case 3) | 17 | 7 | 17 | 13 |
| | 17 | 3 | 17 | 13 |
| AES_ML (case 4) | 13 | 17 | 7 | 17 |
| | 13 | 17 | 3 | 17 |
| Simultaneous constriction (case 5) | 7 | 17 | 17 | 7 |
| | 3 | 17 | 17 | 3 |

case are summarized in Table I. The detailed 3D geometry of the vocal folds and vocal tract can be found in the MATLAB script in the supplementary material.

The airflow and sound generation within the glottis and vocal tract were simulated by solving the 3D compressible

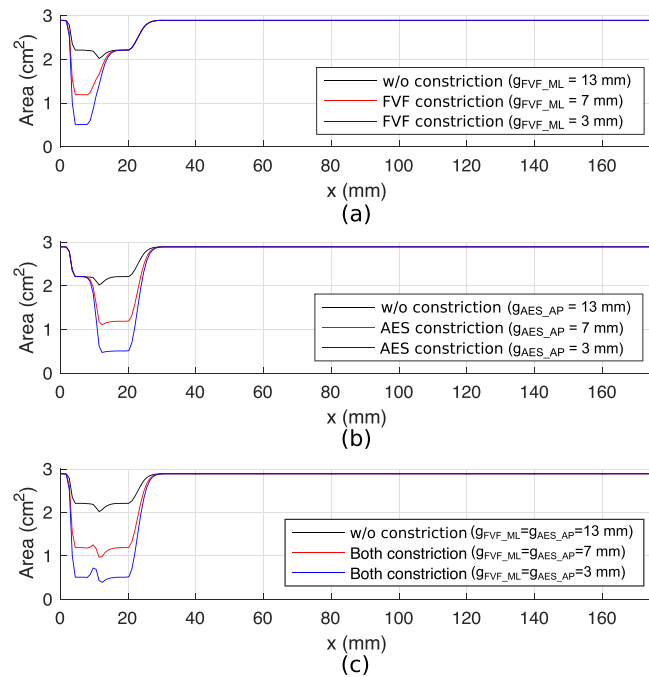


FIG. 2. Cross-sectional area of different vocal tract configurations. (a) Constriction at the level of the false vocal folds alone, (b) constriction at the level of the AES alone, and (c) constriction at the levels of the false folds and AES are displayed. Note that the topmost curves in each panel are identical to each other and correspond to the baseline condition without vocal tract constrictions.

Navier-Stokes equations with a high-order accuracy finite difference method. The volume penalization (VP) method, which is one of the immersed-boundary methods (Liu and Vasilyev, 2007), was employed to treat the moving boundary in the structured computational grids. The VP method adds a penalization term to the governing equations as an external force, modeling solid bodies as highly resistive regions within the computational domain. This approach enables the easy representation of complex moving geometries on structured grids and eliminates the need for explicit boundary tracking. To consider the turbulent flow produced by the glottal gap, large eddy simulation (LES) was applied using a tenth-order-accuracy spatial filter as an implicit turbulence model. The LES computes large-scale turbulent structures while modeling the effects of smaller, subgrid-scale motions. In this study, the spatial filter was employed to control numerical errors and dissipative effects at the subgrid-scale while effectively resolving the turbulence structures. Details of the computational method are reported in Yoshinaga *et al.* (2020).

Two-way fluid-structure interaction was considered in this study. The flow pressure acted as an external force on the two vocal fold masses, and the equation of motion for two masses was solved to predict the vocal fold trajectories as in Ishizaka and Flanagan (1972). In the two-mass model, the masses were permitted to move only in the medial-lateral direction and were connected to the lateral walls with a spring and a damper and to each other with a coupling spring. The updated vocal fold positions and velocities were then imposed as boundary conditions on the fluid simulation at each iterative time step.

The material constants of mass values m , spring constant k , and damping constants r were determined based on the study by Pelorson *et al.* (1994) with $m_1 = 0.17$ g, $m_2 = 0.03$ g, $k_1 = 80$ N/m, $k_2 = 8$ N/m, $k_c = 40$ N/m, $r_1 = 2.33 \times 10^{-2}$ Ns/m, and $r_2 = 1.86 \times 10^{-2}$ Ns/m, respectively. The contact force was calculated as (Ishizaka and Flanagan, 1972)

$$f_{\text{contact}} = -h_i \Delta y (1 + \eta_i \Delta y^2), \quad (1)$$

where Δy is the collision depth. The linear stiffness coefficient h_i was calculated as $h_i = 3k_i$, and the nonlinear coefficient η_i was set to $\eta_1 = \eta_2 = 500/\text{m}^2$. The parameter values used in our study are similar to those proposed by Ishizaka and Flanagan (1972) in their original two-mass model, as well as those used in other recent studies such as Xue *et al.* (2010) and Kaburagi (2011).

A total of approximately 155×10^6 computational grids were constructed for the flow channel. The minimum grid size along the medial-lateral direction near the glottis was set to 0.025 mm, whereas the grid size at epilaryngeal constriction ($x = 10$ mm) was kept smaller than 0.1 mm. The grid-size independence was verified by comparing the results of vocal fold vibrations across five grid resolutions, as reported in Yoshinaga *et al.* (2022). The grid independence of aeroacoustic sound generation is discussed in the supplementary material, where the grid size near the supraglottal constrictions was varied. To resolve the sound

propagation in the computational grids, the time step was set to 0.25×10^{-7} s.

For the boundary conditions, a constant pressure of 1200 Pa was set at the inlet of the pressure chamber [Fig. 1(a)] to simulate phonation with typical loudness. This pressure was increased to 2000 Pa in Sec. III C to investigate the effects of subglottal pressure. A no slip condition was applied to the walls. At the outlet, the no-reflection boundary condition was set with a buffer region to prevent sound reflection from the outlet. After obtaining a stable sustained oscillation, where the peak-to-peak amplitude variation remains within a threshold of 0.1% over time, we continued the simulations for about eight additional glottal cycles to compute the far-field sound spectrum with sufficient frequency resolution. Other voice measures described below were computed using data from the last two cycles.

Apart from the flow simulation, the vocal tract transfer function was calculated for different vocal tract configurations by solving the 3D Helmholtz equation using the multimodal method for acoustic waveguides (Blandin *et al.*, 2015; Yoshinaga *et al.*, 2017). A constant acoustic velocity amplitude was imposed at the glottis, and the transfer function was calculated as the ratio of volume velocities between the lip outlet and the glottis.

To quantify the effects of constriction on voice production, we calculated several voice measures. The glottal resistance was calculated as the ratio between the mean transglottal pressure and the mean glottal flow rate Q_{mean} . The voice source strength or sound pressure level (SPL) at the glottis (SPL_g) was estimated from the time derivative of the glottal flow rate $\partial Q/\partial t$. The normalized maximum flow declination rate (nMFDR) was calculated as the minimum value of

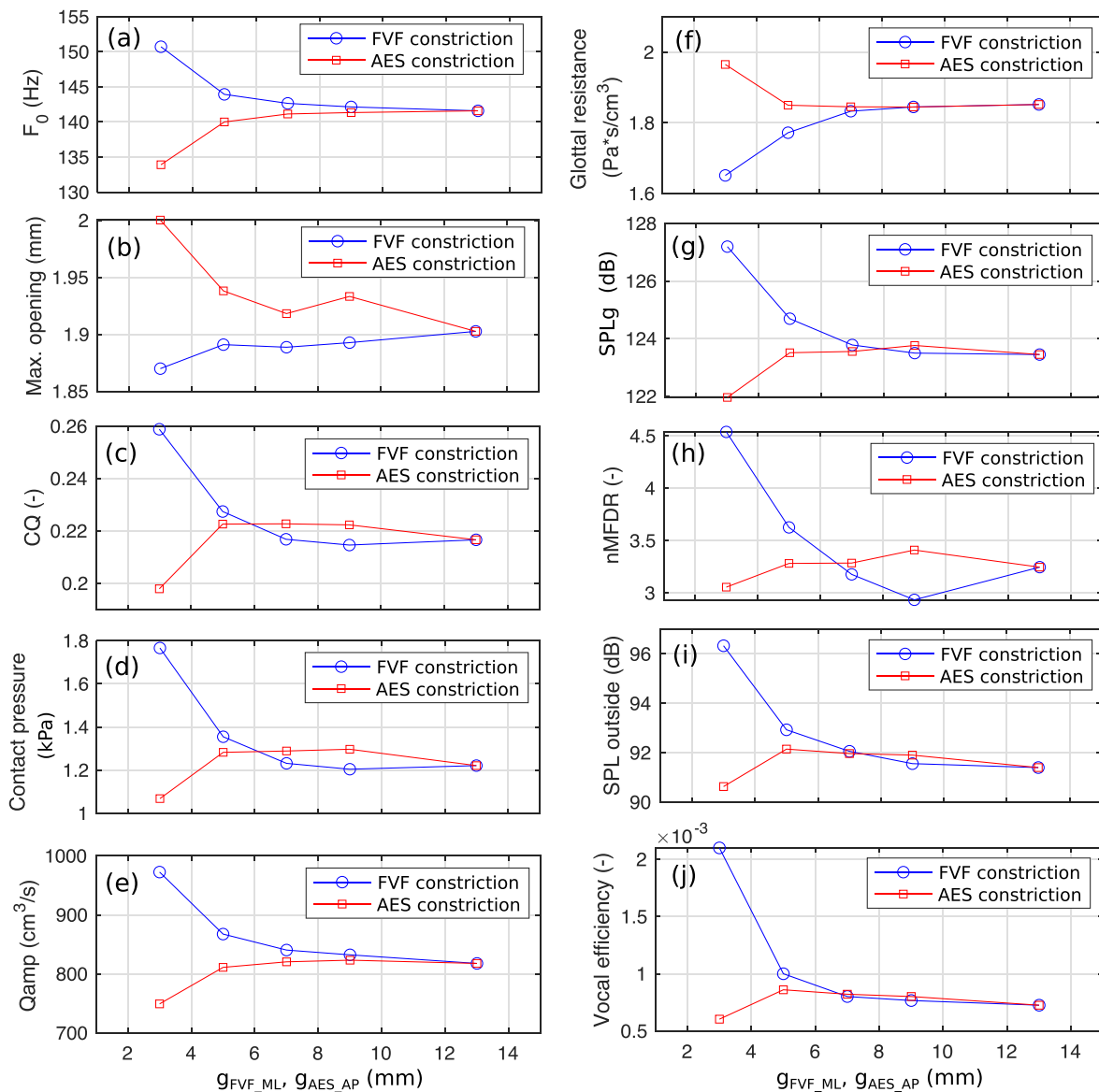


FIG. 3. Voice measures under different constriction degrees of FVF adduction and AES narrowing. (a) Fundamental frequency F_0 , (b) maximum opening of the upper mass, (c) closed quotient (CQ), (d) contact pressure between the upper masses, (e) peak-to-peak amplitude of glottal flow rate Q_{amp} , (f) glottal resistance, (g) SPLs at the glottis SPL_g , (h) normalized maximum flow declination rate, (i) radiated sound pressure levels at 160 mm outside from the vocal tract exit, and (j) vocal efficiency are shown.

$\partial Q/\partial t$ divided by $F_0 Q_{amp}$, where F_0 is the fundamental frequency of the vocal fold vibration and Q_{amp} is the peak-to-peak amplitude of the glottal flow rate. The glottal source spectrum was calculated from the waveform of $\partial Q/\partial t$. The SPL outside of the vocal tract was calculated from the root mean square value of the sound pressure at 160 mm from the vocal tract outlet, with a reference pressure of $20 \mu\text{Pa}$. The vocal efficiency was calculated as the ratio between the acoustic energy at the outside ($x = 160 \text{ mm}$) and the product of the mean subglottal pressure and mean glottal flow rate. Although Titze (2006) noted that this measure is not ideal because of its sensitivity to mouth opening, it remains effective in our study as the mouth opening was kept constant in our vocal tract model. The peak contact pressure was calculated as the maximum force calculated by Eq. (1) divided by the mass surface area $d_l l_g$, where l_g is the glottal length ($l_g = 17 \text{ mm}$). The Reynolds number $Re = Q_{amp} l_g \nu$ in this study varied from 2897 to 3813, where ν is the kinematic viscosity of air.

III. RESULTS

A. Effects of FVF and AES constriction alone (cases 1 and 2)

The voice measures at different degrees of constrictions of the FVFs and AES are plotted in Fig. 3. The effects of FVF and AES constrictions on the voice source were generally small except for the most constricted condition (constriction gap of 3 mm). For example, for constriction gaps of

5 mm or more, F_0 varied within 3 Hz; changes in the closed quotient (CQ) were on the order of 0.01; the peak contact pressure varied within 0.1 kPa; and changes in SPL_g at the glottis were within 1 dB. These changes are relatively small compared to typical variations in normal phonation (Zhang, 2016).

For the most constricted conditions with a constriction gap of 3 mm, changes resulting from the constriction were much larger, particularly for a constriction of 3 mm at the level of the FVFs. The SPL_g , outside SPL, and the vocal efficiency rapidly increased as the FVF gap decreased from $g_{FVF_ML} = 5$ to 3 mm. In addition, the peak contact pressure of vocal folds increased by 0.4 kPa with this increase in FVF constriction. In contrast, changes in Q_{amp} , SPL at the glottis, and outside SPL because of AES constrictions were smaller than those for FVF constrictions. As a result, the vocal efficiency with the AES constriction was almost the same as that without the constriction ($g_{AES_AP} = 13 \text{ mm}$). In general, FVF and AES constrictions had opposite effects on voice production.

The voice source harmonic spectrum, vocal tract transfer function, and outside sound spectrum are depicted in Fig. 4. The voice source spectra remained almost the same for FVF constrictions with gaps of 13 and 7 mm. As the FVF gap decreased from 7 to 3 mm, the source spectral amplitude increased by approximately 8 dB in the frequency range 0.8–3.5 kHz but decreased by about 5 dB at higher frequencies. For the vocal tract transfer function, the first three

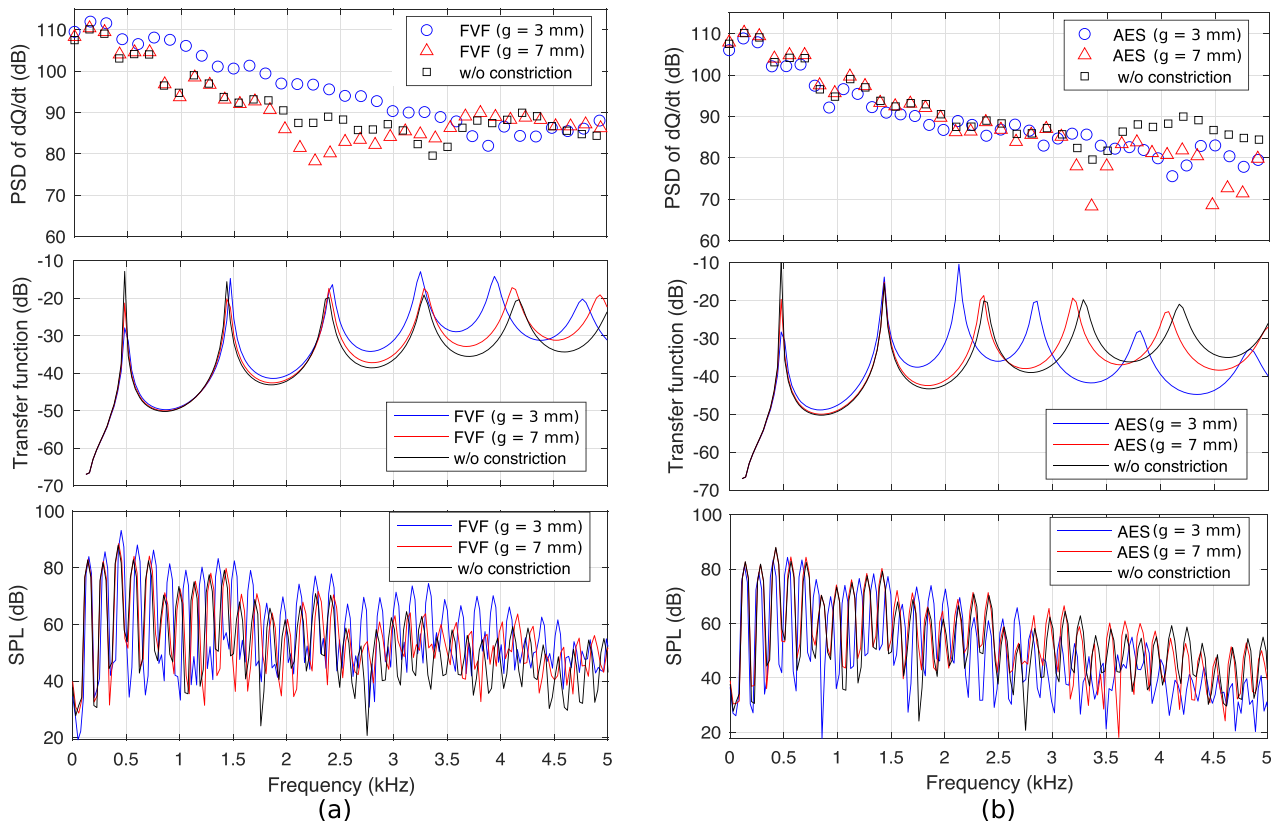


FIG. 4. The voice source spectra (top), vocal tract transfer functions (middle), and spectra of radiated sound outside from the vocal tract (bottom) for different conditions of (a) FVF and (b) AES constriction are displayed.

formants remained almost unchanged, whereas the amplitudes of the fourth and fifth formants were increased by about 6 dB and both formants were shifted to a lower frequency. As a result, the outside voice spectral amplitude was increased by 5–15 dB in the frequency range from 0.8 to 4.5 kHz. In contrast, the voice source and outside sound spectra remained almost the same with the AES constriction in the frequency range up to 3 kHz. Above 3 kHz, the voice source and vocal tract transfer function decreased with constriction, which reduced the outside sound spectra by approximately 10–20 dB.

It should be noted that in this study, the AES constriction was unable to produce a strong formant clustering around 3 kHz as often observed in singers (Sundberg, 1974). This is a result of the relatively large ventricular space in our simulations, which had a significant effect on the higher-order formants, as discussed in the Appendix.

The large changes observed at conditions of extreme FVF constriction (constriction gap of 3 mm) indicate a potential near-field interaction between the FVF and glottal

flow. The flow field and pressure distribution in the glottal and supraglottal region for one oscillation cycle are depicted in Fig. 5 for vocal tract configurations without a constriction, with FVF constriction alone, and with AES constriction alone. The time is normalized by the period T of vocal fold oscillation, and $t/T=0$ indicates the beginning of the closed phase of the glottal cycle. The pressure was sampled at the centerline of flow fields. Videos of flow fields with FVF and AES constrictions are included in the supplementary material. When there was no constriction [Fig. 5(a-1)], the jet flow exited the glottis toward one side of the vocal tract channel. In contrast, with FVF constriction [Fig. 5(a-2)], the jet left the glottis straight and passed through the FVF gap. This jet-straightening effect was reported earlier by Zheng *et al.* (2009), Xue and Zheng (2017), and Kniesburges *et al.* (2017). With AES constriction, the glottal jet exited to one side, similar to that without any constriction, before impinging on the AES, and flow recirculation was observed in the region below the AES constriction. With FVF constriction, the flow pressures in the glottal

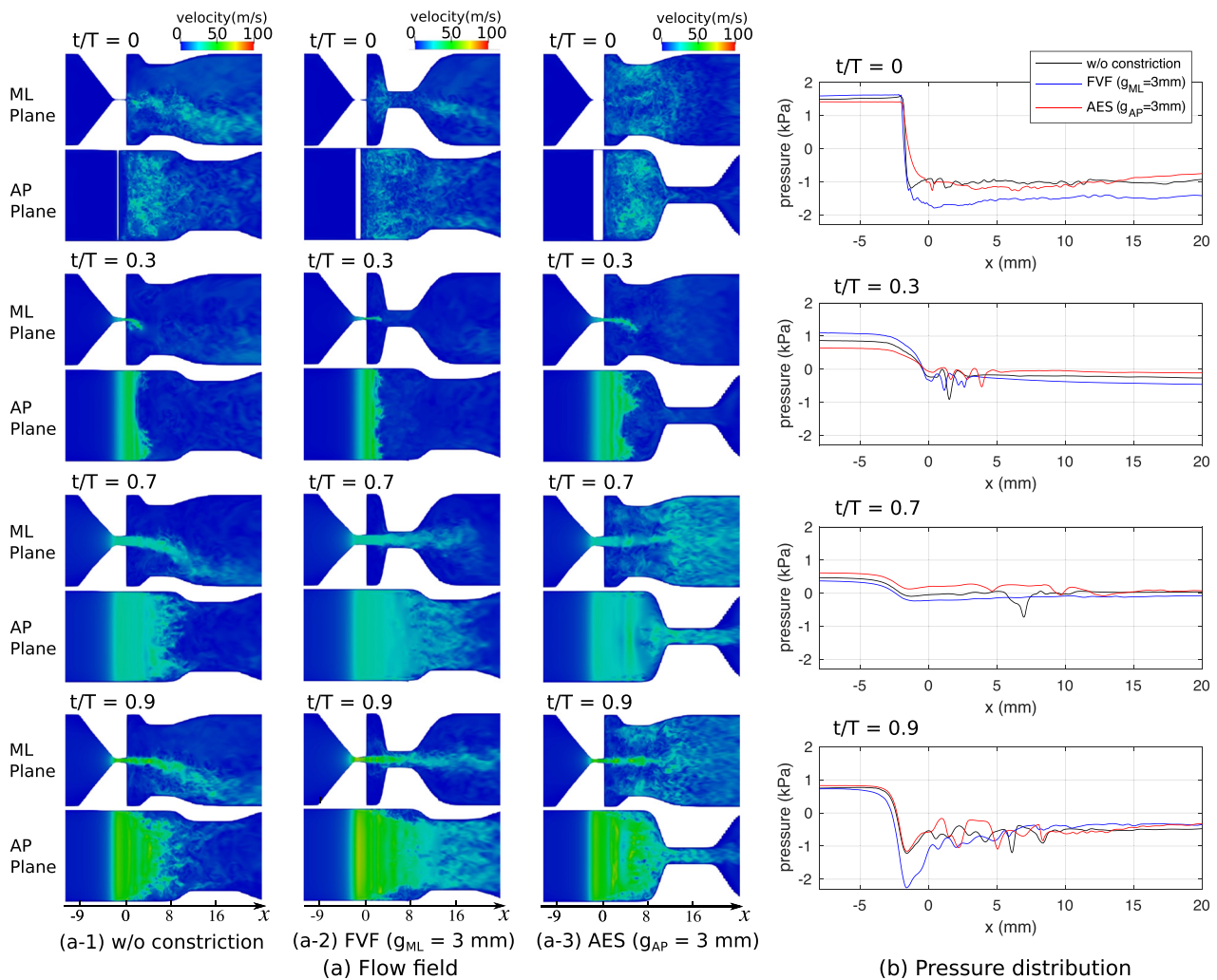


FIG. 5. (a) Glottal and supraglottal flow field in the medial-lateral (ML) and anterior-posterior (AP) planes and (b) pressure distribution at $t/T=0, 0.3, 0.7,$ and 0.9 . Each plane of the flow field was cut at the center of the vocal tract, and the pressure distribution was plotted along the glottal and vocal tract centerline.

region ($x = -2$) and supraglottal region ($x = 5$ mm) were lower than the other two conditions (without any constriction or with AES constriction only) during the closing phase ($t/T = 0.7-1.0$). This indicates that FVF adduction, which constricts the flow from the medial-lateral direction, was able to maintain the high jet velocity exiting the glottis as the jet moved further downstream into the vocal tract, which reduced the supraglottal pressure immediately downstream of the vocal folds. In contrast, when the jet flow was restricted by AES narrowing alone or spread without constriction, the jet velocity decreased rapidly, which led to a higher supraglottal pressure.

The waveforms of the glottal area, glottal flow Q , subglottal pressure at $x = -10$ mm, supraglottal pressure at $x = 1$ mm, and transglottal pressures are plotted in Fig. 6. The subglottal and supraglottal pressures were measured at the center of the y - z plane. The transglottal pressure was calculated as the difference between the subglottal and supraglottal pressures. The three ripples observed in the subglottal pressure [Fig. 6(c)] were caused by acoustic

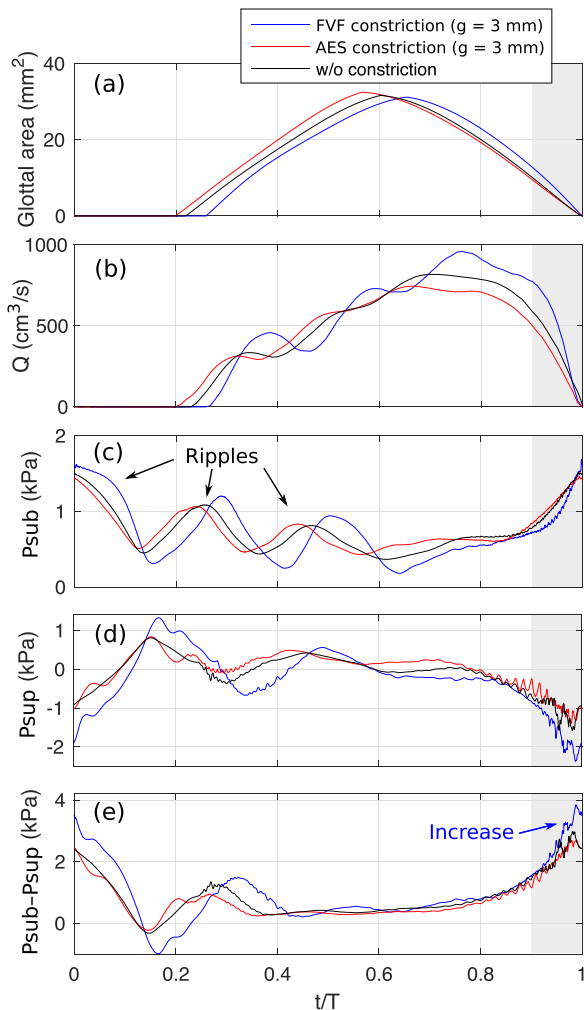


FIG. 6. Waveforms of (a) glottal area, (b) glottal flow rate Q , (c) subglottal pressure ($x = -10$ mm), (d) supraglottal pressure ($x = 1$ mm), and (e) transglottal pressure for conditions without a constriction, with FVF constriction, and with AES constriction are shown. The gray part indicates the closing phase of vocal folds ($t/T = 0.9-1.0$).

reflections, similar to those reported in Yoshinaga *et al.* (2022). During the closing phase ($t/T = 0.9-1.0$), the transglottal pressure was higher for the condition with FVF constriction than that with AES constriction or without a constriction. This results from the straightened jet with FVF constriction (Fig. 5), which lowered the supraglottal pressure. This larger transglottal flow resulted in a higher flow rate and higher rate of flow decrease [i.e., maximum flow declination rate (MFDR)] in the condition with FVF constriction. It should be noted that the transglottal pressure for conditions with AES constriction was almost the same as that in the condition without a constriction, suggesting that AES narrowing had almost no influence on the glottal and supraglottal aerodynamic pressure fields. This means that the effect of AES narrowing was mainly on the vocal tract transfer function as shown in Fig. 4(b).

B. Effects of constriction location and orientations (cases 3 and 4)

In Sec. III A, significant changes in the glottal source were observed only with FVF constriction, where $g_{\text{FVF,ML}} = 3$ mm, but not for conditions with AES constriction. In this section, we elucidate whether these large effects of FVF constriction were because the FVF constriction was closer to the vocal folds or because the FVFs constricted the flow from the medial-lateral direction. Simulations were performed with constrictions at the level of the FVFs to constrict the airway from the anterior-posterior direction (case 3) and constrictions at the level of the AES to constrict the airway from the medial-lateral directions (case 4). The results of voice outcomes are depicted in Fig. 7. Overall, the tendency of voice production changes depended mainly on the constriction orientation rather than the location of the constriction (or distance to the glottis). For example, the SPL_g and SPL of the radiated sound outside the vocal tract were increased when the vocal tract was constricted from the medial-lateral constrictions, whether it was constricted at the levels of FVFs or AES. In contrast, both SPLs were decreased by anterior-posterior constrictions at the levels of either the FVFs or AES. Similarly, other measures, such as the glottal resistance, vocal efficiency, and contact pressure, were increased or decreased from the case without a constriction depending mainly on the constriction orientation rather than the location.

On the other hand, the constriction location determined the magnitude of the effects: the closer the constriction was to the vocal folds, the stronger the effects were in the extreme constriction conditions (i.e., $g_{\text{FVF}} = 3$ mm or $g_{\text{AES}} = 3$ mm). The F_0 , CQ, and SPLs were increased or decreased more by the constrictions at the levels of the FVFs than at the level of the AES. It should be noted that when the gap was 7 mm for medial-lateral constrictions, the effects of the constriction at the level of the AES were stronger than those at the level of the FVFs. This is probably because the wider constriction ($g_{\text{AES}} = 7$ mm) was able to maintain the high jet velocities over a larger distance.

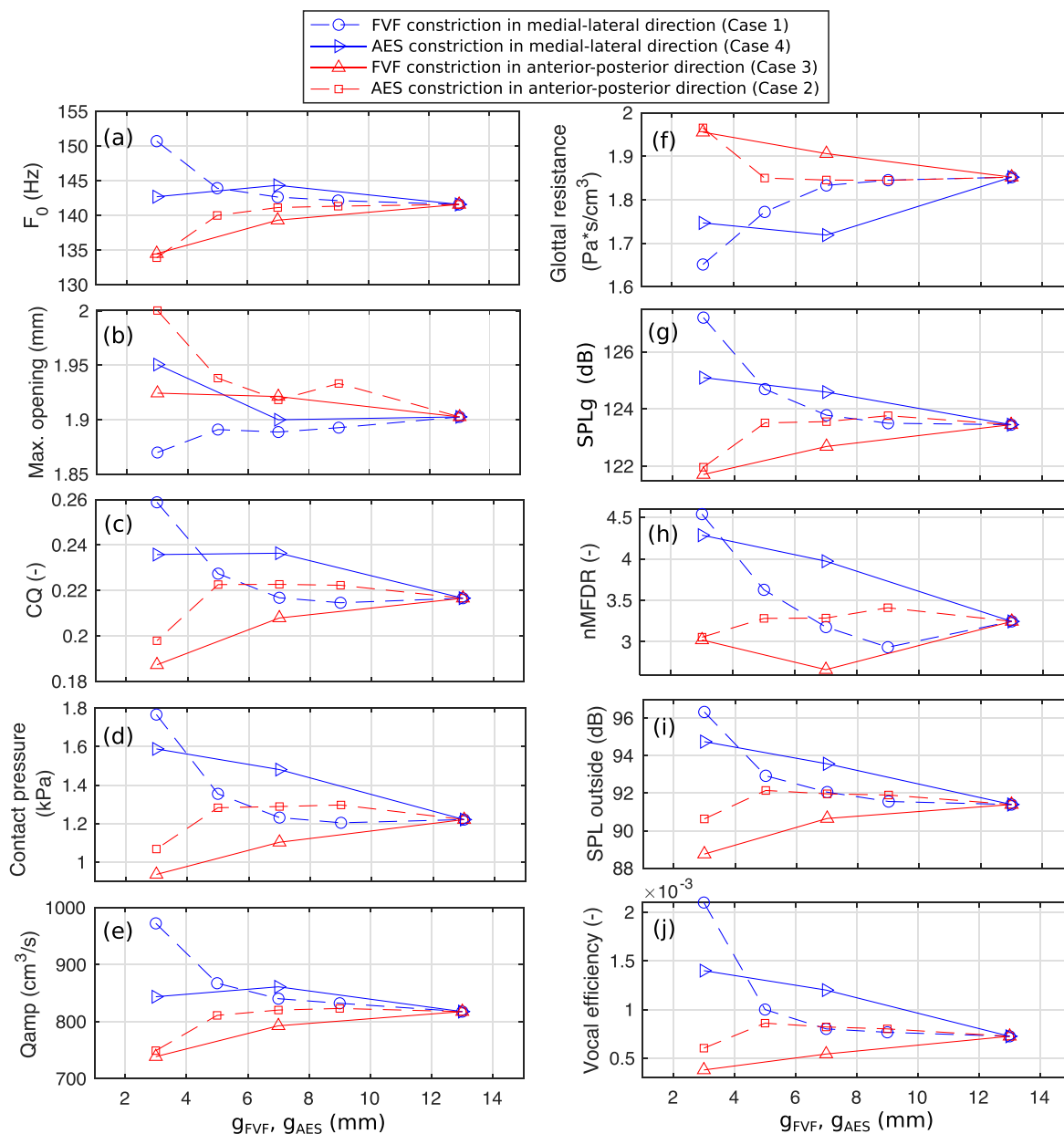


FIG. 7. Voice outcome measures for conditions of FVF and AES constriction with different constriction orientations. (a) Fundamental frequency F_0 , (b) maximum opening of upper mass, (c) CQ, (d) contact pressure of upper mass, (e) peak-to-peak amplitude of glottal flow rate Q_{amp} , (f) glottal resistance, (g) SPL at the glottis SPL_g , (h) normalized maximum flow declination rate, (i) SPL at 160 mm outside from the vocal tract exit, and (j) vocal efficiency are displayed.

This suggests that the magnitude of the effects may depend on the ratio between the constriction gap and the jet width, which also depends on the distance from the vocal folds.

C. Effects of subglottal pressure in cases 1 and 2

Selected voice measures as a function of the constriction gap for subglottal pressures of 1.2 and 2 kPa are shown in Fig. 8 for cases 1 (FVF constriction only) and 2 (AES constriction only). The general trends of changes are similar for both subglottal pressure values: the effects of FVF and AES constrictions were generally smaller except for the most constricted condition with a constriction gap of 3 mm.

Whereas the fundamental frequency and CQ under $P_s=2.0$ kPa were in the similar range to those of $P_s=1.2$ kPa, the other measures, including the maximum opening, glottal flow rates, SPL_g , and radiated outside SPL, were significantly increased by the subglottal pressure. This increase was much larger than the increases observed as a result of FVF or AES constriction alone, including the most extreme FVF constriction with a gap of 3 mm. This is in agreement with the previous simulations, showing that the effects of vocal tract constriction on the voice source are much smaller than those of the subglottal pressure and vocal fold configurations (Zhang, 2023). This is particularly the case for the peak vocal fold contact pressure, which almost

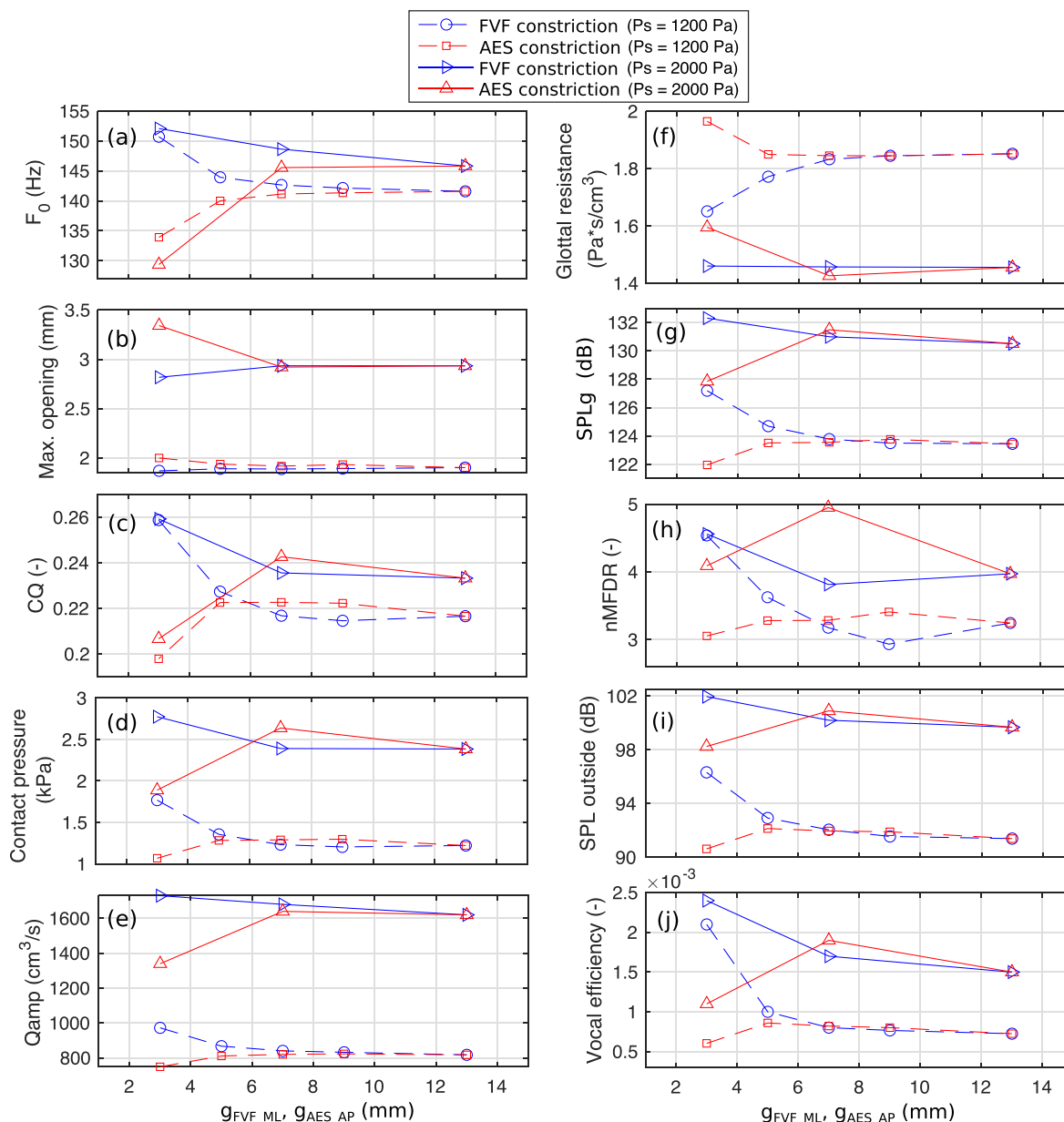


FIG. 8. Effect of subglottal pressure on voice outcome measures. (a) Fundamental frequency F_0 , (b) maximum opening of upper mass, (c) CQ, (d) contact pressure of upper mass, (e) peak-to-peak amplitude of glottal flow rate Q_{amp} , (f) glottal resistance, (g) SPL at the glottis SPL_g , (h) normalized maximum flow declination rate, (i) SPL at 160 mm outside from the vocal tract exit, and (j) vocal efficiency are shown.

doubled with increasing pressure but varied only slightly with the degree of vocal tract constriction.

D. Effects of simultaneous FVF and AES constrictions (case 5)

The effects of simultaneous FVF and AES constrictions were investigated in case 5 and compared to conditions with FVF or AES constriction alone (Fig. 9). Such simultaneous FVF and AES constrictions are often observed in, for example, muscle tension dysphonia (Zhang, 2021c). Overall, changes resulting from simultaneous constrictions were within the range of changes caused by FVF or AES constriction alone. Measures of

vocal fold vibration (i.e., F_0 , maximum opening, CQ) in the simultaneous constriction cases varied in a similar manner to those observed with AES constriction alone. This suggests that AES constriction had a more dominant effect than FVF constriction on vocal fold dynamics. Meanwhile, the radiated SPL and vocal efficiency increased slightly with simultaneous constrictions. These increases were larger than those with AES constriction alone but smaller than those observed with FVF constriction alone. These results indicate that with simultaneous FVF and AES constrictions, the influence of FVF constriction on the airflow and sound generation was masked to some degree by that of AES constriction, which increased glottal resistance and weakened source-filter interaction.

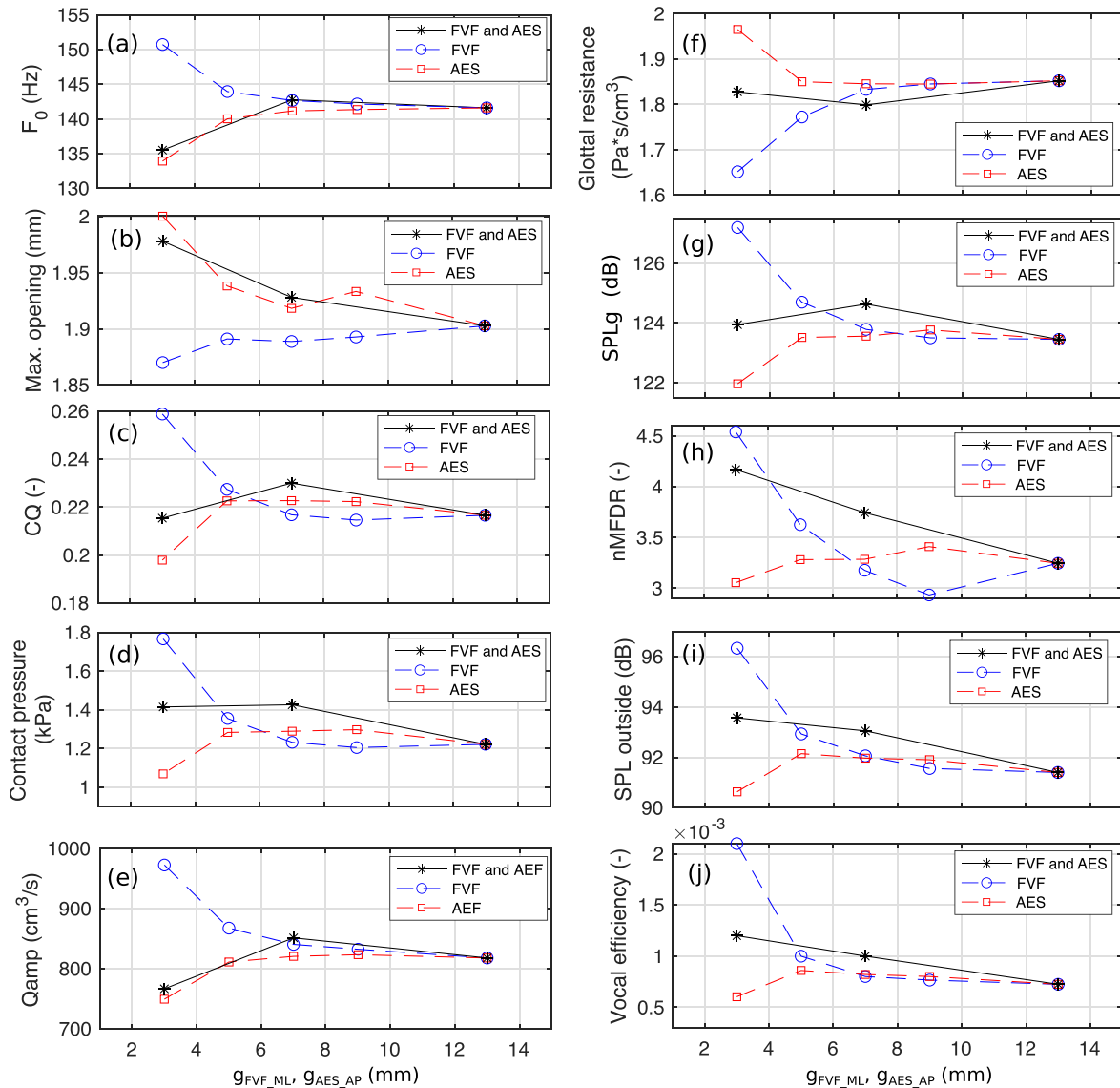


FIG. 9. Voice outcomes with simultaneous constriction at levels of the FVFs and AES. The results from conditions with FVF or AES constriction alone are plotted with dotted lines. (a) Fundamental frequency F_0 , (b) maximum opening of upper mass, (c) CQ, (d) contact pressure of upper mass, (e) peak-to-peak amplitude of glottal flow rate Q_{amp} , (f) glottal resistance, (g) SPL at the glottis SPL_g , (h) normalized maximum flow declination rate, (i) SPL at 160 mm outside from the vocal tract exit, and (j) vocal efficiency are displayed.

IV. DISCUSSION

The goal of this study is to investigate to what extent epilaryngeal constriction improves the voice source. Our results showed that the vocal fold vibration amplitude, glottal flow amplitude, and vocal efficiency increased when the FVFs were tightly adducted, which is similar to the observation in Zheng *et al.* (2009). However, the improvement in vocal efficiency was only observed for the extremely small gap ($g_{FVF} = 3$ mm) in our study, suggesting a more limited role of supraglottal constriction in improving vocal efficiency. This result is consistent with the tendency observed in the 1D flow simulation coupled with a 3D finite element vocal fold model (Zhang, 2023). For example, Zhang (2023) reported changes of approximately 7 Hz in F_0 , 0.03 in CQ, $100 \text{ cm}^3/\text{s}$ in Q_{amp} , and 0.5 in nMFDR. In comparison, our simulations, excluding extreme FVF constriction, showed

changes of approximately 8 Hz in F_0 , 0.02 in CQ, $70 \text{ cm}^3/\text{s}$ in Q_{amp} , and 0.4 in nMFDR.

Agarwal *et al.* (2003) reported that the FVF gap ranged from 2.3 to 8.3 mm in eight males and 2.0 to 7.0 mm in five females for untrained subjects in modal and falsetto conditions. The 3 mm gap of this study, where significant effects on the voice source were observed, falls within the lower end of these ranges. Therefore, the results of this study indicate that the effect of epilaryngeal narrowing on the voice source is generally small in normal phonation, particularly when compared to the effects of subglottal pressure and vocal fold configurations. However, this effect may become important in pathological conditions involving strong compensatory supraglottal adduction or certain singing techniques that explore extreme supraglottal constriction.

Note that in this study, the FVFs were rigid and their potential involvement in vibration was not considered. In humans, when strongly adducted, the FVFs may be induced into vibration, as observed in certain phonatory tasks, such as throat singing (e.g., Sakakibara *et al.*, 2001; Bailly *et al.*, 2010). Bailly *et al.* (2010) showed that the estimated maximum aperture of oscillating FVFs was approximately 2.5 mm. Thus, FVFs with a 3 mm gap might also vibrate. It is unclear whether the observed increase in vocal efficiency at a 3-mm FVF gap in this study would remain in the presence of FVF oscillation, which needs to be investigated in a future study.

The significant effects on voice production when the FVF constriction was narrowed to a gap of $g_{\text{FVF_ML}} = 3$ mm was achieved by a combination of an increase in the source magnitude resulting from the source-filter interaction and the improved vocal tract transfer function. For this condition, the ratio between the maximum glottal gap and constriction gap was approximately 3 mm, and this agrees with the range of glottal resistance reduction observed in Agarwal *et al.* (2004). While Agarwal *et al.* (2003) and Agarwal *et al.* (2004) focused on experimental measurements, our flow simulations provide additional insight into the aerodynamic mechanisms underlying this phenomenon. Specifically, we found that constricting the jet flow from the medial-lateral direction allowed the jet to persist longer into the supraglottal region and maintain a higher jet velocity, thus reducing the back pressure immediately above the vocal folds and increasing the transglottal pressure. In contrast, constricting the jet from the anterior-posterior direction did not have this effect on the supraglottal jet. As a result, the transglottal pressure was almost the same as that without a supraglottal constriction, and AES constriction had almost no influence on the voice source.

The fact that the effects of epilaryngeal constrictions of varying configurations (location and orientation) were small indicates a small effect of the 3D flow features on voice production. Thus, these 3D features can be neglected in phonation models when the constriction gap is larger than 3 mm. The only constriction condition in which significant disagreements were observed between 1D and 3D flow simulations was the condition with a FVF constriction gap of 3 mm. For this case, the constriction orientation and its impact on the jet flow should be considered to accurately capture the source-filter interaction effects. It should be noted that a two-mass vocal fold model was used in this study. Although this model has been widely used in voice research, it simplifies the complex continuum mechanics of vocal fold motion, limiting direct experimental validation. Future work should aim to validate findings of this study in experiments or simulations that better model the 3D vocal fold mechanics.

The AES constriction in this study showed a slight decrease in the output voice SPL as well as vocal efficiency, especially at frequencies above 3 kHz. Moreover, the effects of simultaneous FVF and AES constrictions on the output

SPL were also small. This contradicts previous observations that AES constriction increases the harmonic energy around 3 kHz because of the singer's formant clustering (Sundberg, 1974; Yanagisawa *et al.*, 1989). This difference is mainly caused by the relatively large ventricular depth in this study. When the ventricular depth was simultaneously reduced with AES constriction, we were able to significantly boost formants F3–F5 around 3 kHz, as shown in the Appendix. Similar effects of reducing the ventricle space on the acoustic output have also been reported in Honda *et al.* (2010), and these results suggest that proper tuning of the epilaryngeal space is important to increase the output voice efficiency. To further improve the physiological relevance of the model, future studies should incorporate speaker-specific laryngeal and epilaryngeal geometry.

V. CONCLUSIONS

In this study, we conducted 3D numerical flow simulations coupled with a two-mass vocal fold model to clarify to what extent the 3D glottal/supraglottal jet flow and voice source are influenced by FVF and AES constrictions. The results demonstrated that the overall effects of FVF and AES constrictions on the voice source and vocal fold contact pressures were relatively small, particularly when compared to the effects of varying subglottal pressure. However, notable increases in the voice efficiency were observed when the FVFs were strongly adducted to a constriction gap of 3 mm. This improvement was because FVF adduction constricted the supraglottal jet from the medial-lateral direction and allowed the jet to persist longer and maintain a higher jet velocity, thus increasing transglottal pressure and voice source strength. In contrast, AES narrowing constricted the airflow from the anterior-posterior direction and had only small influence on the glottal and supraglottal pressure fields and the voice source. These results indicate that the main effect of epilaryngeal adjustments on voice production is their impact on the vocal tract transfer function rather than their impact on the voice source.

SUPPLEMENTARY MATERIAL

See the [supplementary material](#) for the MATLAB code of vocal tract and vocal fold geometry (SuppPub1.m), the grid independency analysis (SuppPub2.pdf), and video files for flow and acoustic fields with FVF constriction alone (SuppPub3.mp4) and AES constriction alone (SuppPub4.mp4).

ACKNOWLEDGMENTS

This study was supported by Japan Society for the Promotion of Science, Grant-in-Aid for Scientific Research (JSPS KAKENHI) (Grant Nos. JP23K17195 and JP22KK0238), Research Grant No. R01DC020240 from the National Institute on Deafness and Other Communication Disorders, the National Institutes of Health, and an Institute of Digital Research and Education (IDRE) Fellowship,

University of California, Los Angeles (UCLA). This work used the computational resources of the Fugaku supercomputer provided by the RIKEN Center for Computational Science through the High Performance Computing Infrastructure (HPCI) System Research Project (Project Identification No. hp240007).

AUTHOR DECLARATIONS

Conflict of Interest

The authors have no conflicts to disclose.

DATA AVAILABILITY

The data that support the findings of this study are available from the corresponding author upon reasonable request.

APPENDIX: ACOUSTIC EFFECTS OF VENTRICULAR SPACE

The acoustic effects of the ventricular depth in the current simplified vocal tract were examined. When the AES was narrowed from $g_{AES_AP} = 13\text{--}3\text{ mm}$ [Fig. 4(b)], the frequencies of third to fifth formants were decreased, and the amplitudes of fifth formants were reduced by approximately 6 dB. However, when the ventricular space and FVF gap were simultaneously narrowed with the AES (Fig. 10), the formant frequencies were shifted to higher values, and the amplitudes of fourth and fifth formants were increased by 7–19 dB. This result is consistent with the acoustic analysis in Zhang (2023) with a similar vocal tract geometry and indicates that simultaneous narrowing of the FVFs, ventricular cavity and AES is necessary to achieve the singer’s formant clustering (Sundberg, 1974) or the “ringing voice” quality (Yanagisawa *et al.*, 1989).

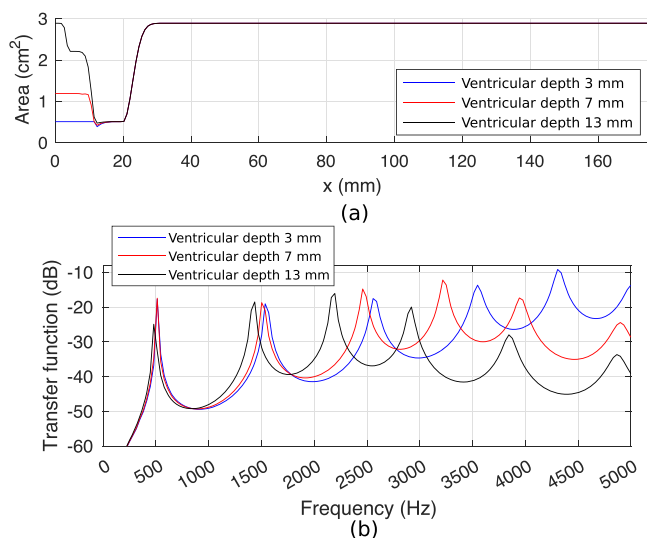


FIG. 10. Vocal tract area functions (a) and the corresponding vocal tract transfer functions (b) with and without simultaneous narrowing of the ventricular cavity are shown.

Agarwal, M., Scherer, R. C., and Hollien, H. (2003). “The false vocal folds: Shape and size in frontal view during phonation based on laminagraphic tracings,” *J. Voice* **17**(2), 97–113.

Agarwal, M., Scherer, R. C., and Witt, K. J. (2004). “The effects of the false vocal folds on translaryngeal airflow resistance,” in *Proceedings of the International Conference on Voice Physiology and Biomechanics*, Marseille, France (August 18–20, 2004), pp. 1–6.

Alipour, F., Jaiswal, S., and Finnegan, E. (2007). “Aerodynamic and acoustic effects of false vocal folds and epiglottis in excised larynx models,” *Ann. Otol. Rhinol. Laryngol.* **116**(2), 135–144.

Bailly, L., Henrich, N., and Pelorson, X. (2010). “Vocal fold and ventricular fold vibration in period-doubling phonation: Physiological description and aerodynamic modeling,” *J. Acoust. Soc. Am.* **127**(5), 3212–3222.

Bailly, L., Pelorson, X., Henrich, N., and Rutu, N. (2008). “Influence of a constriction in the near field of the vocal folds: Physical modeling and experimental validation,” *J. Acoust. Soc. Am.* **124**(5), 3296–3308.

Blandin, R., Arnela, M., Laboissière, R., Pelorson, X., Guasch, O., Van Hirtum, A., and Laval, X. (2015). “Effects of higher order propagation modes in vocal tract like geometries,” *J. Acoust. Soc. Am.* **137**(2), 832–843.

Döllinger, M., Berry, D. A., Luegmair, G., Hüttner, B., and Bohr, C. (2012). “Effects of the epilarynx area on vocal fold dynamics and the primary voice signal,” *J. Voice* **26**(3), 285–292.

Farahani, M. H., Mousel, J., Alipour, F., and Vigmostad, S. (2013). “A numerical and experimental investigation of the effect of false vocal fold geometry on glottal flow,” *J. Biomech. Eng.* **135**(12), 121006.

Farbos de Luzan, C., Chen, J., Mihaescu, M., Khosla, S. M., and Gutmark, E. (2015). “Computational study of false vocal folds effects on unsteady airflows through static models of the human larynx,” *J. Biomech.* **48**(7), 1248–1257.

Honda, K., Kitamura, T., Takemoto, H., Adachi, S., Mokhtari, P., Takano, S., Nota, Y., Hirata, H., Fujimoto, I., Shimada, Y., Masaki, S., Fujita, S., and Dang, J. (2010). “Visualisation of hypopharyngeal cavities and vocal-tract acoustic modelling,” *Comput. Methods Biomech. Biomed. Eng.* **13**(4), 443–453.

Ishizaka, K., and Flanagan, J. L. (1972). “Synthesis of voiced sounds from a two-mass model of the vocal cords,” *Bell Syst. Tech. J.* **51**(6), 1233–1268.

Jelinger, J., Perta, K., Lee, J., Wiksten, N., and Bae, Y. (2024). “Oropharyngeal and aryepiglottic narrowing for twang: A magnetic resonance imaging study,” *J. Voice* (published online).

Kaburagi, T. (2011). “Voice production model integrating boundary-layer analysis of glottal flow and source-filter coupling,” *J. Acoust. Soc. Am.* **129**(3), 1554–1567.

Kniesburges, S., Birk, V., Lodermeier, A., Schützenberger, A., Bohr, C., and Becker, S. (2017). “Effect of the ventricular folds in a synthetic larynx model,” *J. Biomech.* **55**, 128–133.

Kucinschi, B. R., Scherer, R. C., DeWitt, K. J., and Ng, T. T. M. (2006). “Flow visualization and acoustic consequences of the air moving through a static model of the human larynx,” *ASME J. Biomech. Eng.* **128**(3), 380–390.

Liu, Q., and Vasilyev, O. V. (2007). “A Brinkman penalization method for compressible flows in complex geometries,” *J. Comput. Phys.* **227**(2), 946–966.

Mihaescu, M., Khosla, S. M., and Ephraim, G. J. (2013). “Quantification of the false vocal-folds effects on the intra-glottal pressures using large eddy simulation,” *Proc. Mtgs. Acoust.* **19**, 060302.

Moisik, S. R., and Esling, J. H. (2014). “Modeling the biomechanical influence of epilaryngeal stricture on the vocal folds: A low-dimensional model of vocal–ventricular fold coupling,” *J. Speech. Lang. Hear. Res.* **57**(2), S687–S704.

Pelorson, X., Hirschberg, A., van Hassel, R. R., Wijnands, A. P. J., and Auregan, Y. (1994). “Theoretical and experimental study of quasisteady-flow separation within the glottis during phonation. Application to a modified two-mass model,” *J. Acoust. Soc. Am.* **96**(6), 3416–3431.

Sadeghi, H., Döllinger, M., Kaltenbacher, M., and Kniesburges, S. (2019). “Aerodynamic impact of the ventricular folds in computational larynx models,” *J. Acoust. Soc. Am.* **145**(4), 2376–2387.

Sakakibara, K. I., Imagawa, H., Kouishi, T., Kondo, K., Murano, E. Z., Kumada, M., and Niimi, S. (2001). “Vocal fold and false vocal fold vibrations in throat singing and synthesis of khöömei,” in *Proceedings of the*

- International Computer Music Conference*, Havana, Cuba (September 18–22, 2001), pp. 1–4.
- Stevens, K. N. (1998). *Acoustic Phonetics* (MIT Press, Cambridge, MA).
- Sundberg, J. (1974). “Articulatory interpretation of the ‘singing formant,’” *J. Acoust. Soc. Am.* **55**(4), 838–844.
- Takemoto, H., Adachi, S., Kitamura, T., Mokhtari, P., and Honda, K. (2006). “Acoustic roles of the laryngeal cavity in vocal tract resonance,” *J. Acoust. Soc. Am.* **120**(4), 2228–2238.
- Titze, I. R. (2006). “Voice training and therapy with a semi-occluded vocal tract: Rationale and scientific underpinnings,” *J. Speech Lang. Hear. Res.* **49**, 448–459.
- Titze, I. R., and Story, B. H. (1997). “Acoustic interactions of the voice source with the lower vocal tract,” *J. Acoust. Soc. Am.* **101**(4), 2234–2243.
- Titze, I. R., and Worley, A. S. (2009). “Modeling source-filter interaction in belting and high-pitched operatic male singing,” *J. Acoust. Soc. Am.* **126**(3), 1530–1540.
- Xue, Q., Mittal, R., Zheng, X., and Bielamowicz, S. (2010). “A computational study of the effect of vocal-fold asymmetry on phonation,” *J. Acoust. Soc. Am.* **128**(2), 818–827.
- Xue, Q., and Zheng, X. (2017). “The effect of false vocal folds on laryngeal flow resistance in a tubular three-dimensional computational laryngeal model,” *J. Voice* **31**(3), 275–281.
- Yanagisawa, E., Estill, J., Kmucha, S. T., and Leder, S. B. (1989). “The contribution of aryepiglottic constriction to ‘ringing’ voice quality—A videolaryngoscopic study with acoustic analysis,” *J. Voice* **3**(4), 342–350.
- Yoshinaga, T., Nozaki, K., and Iida, A. (2020). “Hysteresis of aeroacoustic sound generation in the articulation of [s],” *Phys. Fluids* **32**(10), 105114.
- Yoshinaga, T., Van Hirtum, A., and Wada, S. (2017). “Multimodal modeling and validation of simplified vocal tract acoustics for sibilant/s/,” *J. Sound Vib.* **411**, 247–259.
- Yoshinaga, T., Zhang, Z., and Iida, A. (2022). “Comparison of one-dimensional and three-dimensional glottal flow models in left-right asymmetric vocal fold conditions,” *J. Acoust. Soc. Am.* **152**(5), 2557–2569.
- Zhang, C., Zhao, W., Frankel, S. H., and Mongeau, L. (2002). “Computational aeroacoustics of phonation, Part II: Effects of flow parameters and ventricular folds,” *J. Acoust. Soc. Am.* **112**(5), 2147–2154.
- Zhang, J., Honda, K., Wei, J., and Kitamura, T. (2019). “Morphological characteristics of male and female hypopharynx: A magnetic resonance imaging-based study,” *J. Acoust. Soc. Am.* **145**(2), 734–748.
- Zhang, Z. (2016). “Cause-effect relationship between vocal fold physiology and voice production in a three-dimensional phonation model,” *J. Acoust. Soc. Am.* **139**(4), 1493–1507.
- Zhang, Z. (2021a). “Vocal tract adjustments to minimize vocal fold contact pressure during phonation,” *J. Acoust. Soc. Am.* **150**(3), 1609–1619.
- Zhang, Z. (2021b). “Interaction between epilaryngeal and laryngeal adjustments in regulating vocal fold contact pressure,” *JASA Express Lett.* **1**(2), 025201.
- Zhang, Z. (2021c). “The physical aspects of vocal health,” *Acoust. Today* **17**(3), 60–68.
- Zhang, Z. (2023). “The influence of source-filter interaction on the voice source in a three-dimensional computational model of voice production,” *J. Acoust. Soc. Am.* **154**(4), 2462–2475.
- Zheng, X., Bielamowicz, S., Luo, H., and Mittal, R. (2009). “A computational study of the effect of false vocal folds on glottal flow and vocal fold vibration during phonation,” *Ann. Biomed. Eng.* **37**, 625–642.